Measurement of the quenching of spontaneous emission coefficients in laser-produced plasmas

Y. Chung, H. Hirose,* and S. Suckewer†
Princeton Plasma Physics Laboratory, P.O. Box 451, Princeton, New Jersey 08543
(Received 1 May 1989; revised manuscript received 6 July 1989)

The quenching of Einstein A coefficients was observed by measuring the branching ratio of visible and extreme-ultraviolet line intensities for C IV, C III, and N V ions.

I. INTRODUCTION

Since the formula for the Einstein A coefficient was derived in the pioneering works of Weisskopf and Wigner[1] (WW) based on Dirac's theory of light, it has been widely accepted as valid in any practically important cases. In essence, the expression WW obtained was the same as that for a classical oscillating dipole, except that the quantum-mechanical dipole-moment matrix element between the upper and the lower level of transition replaced the classical dipole moment. They also assumed an exponential decrease for the excitation probability of the upper state as an *Ansatz* and proved it *a posteriori*.

However, the derivation of the Einstein A coefficient has often been the subject of rigorous theoretical investigation on the basis of other theories of light.[2,3] Even though essentially the same expressions as that of WW were obtained, it strongly suggests that the nature of radiative transition is not yet fully known. It was also noted by several authors[4–7] that the rate of spontaneous radiative decay can deviate significantly from the Weisskopf-Wigner expression in certain environments where the atoms are located. Most notably, the spontaneous emission of radiation by an excited atom is completely suppressed in a cavity whose characteristic dimension is less than half the wavelength of the photon. It is believed that this effect is related to the decoupling of the vacuum field and the radiating atom. In quantum electrodynamics (QED), the excited atom is driven to emit a photon and decay to a lower state by the fluctuation in the vacuum field if the atom is located in free space or a cavity whose dimension is much larger than the radiation wavelength. As the dimensions of the cavity become small compared to the radiation wavelength, the density of modes accessible to the atom decreases significantly. In this situation, the excited atom can no longer decay as freely as in the large cavity, and the radiative transition is effectively suppressed. A similar effect was also observed in the cyclotron radiation of an electron confined in a Penning trap[8] and has been predicted in solid-state cavities.[9]

In a previous work,[10] the observation that the branching ratio of two radiative transitions originating from the same upper level decreased by about an order of magnitude at an electron density of around 10^{19} cm^{-3} compared to the ratio at 10^{18} cm^{-3} led us to the conclusion that the coefficients of spontaneous emission were not constants. The term "branching ratio" in this paper denotes the ratio of the experimentally measured intensities of the visible and the xuv (extreme ultraviolet) light unless specified otherwise. The branching ratios were measured with a novel xuv-visible duomultichannel spectrometer. The spontaneous-emission intensity I_{nm} (in photons) for the transition $n \rightarrow m$ is proportional to the upper-level population density, the A coefficient, and a geometrical factor k, that is,[11]

$$I_{nm} = k_n(r) N_n(N_e, T_e) A_{nm} \ . \quad (1)$$

Hence, the branching ratio for optically thin plasmas is the same as the ratio of the corresponding A coefficients. Therefore, if the A coefficients are constant and independent of the electron density or other environmental factors, the branching ratio should remain constant even as we observe regions of different electron density in the plasma. It was our primary finding that this was not true.

The observed change in the branching ratio could be attributed to the following reasons: (1) self-absorption of the visible light; (2) cutoff of the visible light in a region of high electron density where the plasma frequency $\nu_p = (N_e e^2/m\pi)^{1/2}$ is larger than the visible light frequency ν_{vis}; (3) refraction of the visible light out of the spectrometer line of sight; (4) improper alignment of the spectrometers; (5) stimulated emission of the xuv light at a level comparable to the spontaneous emission; (6) nonlinear detector sensitivity at low and high intensities; (7) other experimental errors, including misinterpretation of the data; and (8) deviation of the spontaneous-emission coefficients from the vacuum (or low-density) value.

An extremely careful examination, including supplementary testing experiments of the other possibilities [(1)–(7)], confirmed the hypothesis that in higher-density plasmas the spontaneous-emission coefficients decreased. This may be a result of free electrons' interaction with atoms and ions.

In Sec. II, we describe measurements of the changes in the branching ratios of the C IV (312 and 5801–5812 Å), C III (574 and 5696 Å), and N V (209 and 4603–4620 Å) transitions, and recent results obtained from higher-density plasmas produced by a ruby laser. These show an even larger decrease in branching ratio than could be obtained with a CO_2 laser as reported in Ref. 10. In Sec. III, we attempt to explain this phenomenon, and in Sec. IV, we state our conclusions.

II. EXPERIMENT

In this section we describe (1) experimental arrangements, (2) the branching-ratio measurement experiment on CO_2-laser-produced C IV and C III ions, (3) measurement of the branching ratio on ruby-laser-produced C IV ions, (4) measurement of the branching ratio on CO_2-laser-produced N V ions, and (5) measurement of the light attenuation, e.g., by self-absorption and refraction, due to the plasma.

The experimental setup is shown in Fig. 1. The arrangement primarily consists of the lasers, the target chamber, the spectrometers, and the supporting systems, such as vacuum pumps and the data-acquisition system. The ruby laser is on top of the CO_2 laser and the two laser beams run parallel to each other. The CO_2 laser beam is focused onto the target by a NaCl lens of focal length $f=50$ cm, and the ruby laser beam is focused by a quartz lens of focal length $f=25$ cm after being redirected by a periscope into the CO_2 laser-beam axis. The position of the focusing lens for the ruby laser beam can be adjusted up to ± 3 cm to provide optimal conditions for the generation of different ionization stages. The XeCl laser beam is positioned at approximately 45° to the CO_2 laser and the ruby laser. The characteristics of these lasers are summarized in Table I.

The plasma was created by interaction of the laser beam with a solid target in the vacuum chamber. The typical length of the target was 24 mm and each step was 4 mm long. Several targets of various widths ranging from 200 μm to 4 mm were tested in this experiment. Even though narrower targets of width ≈ 200 μm gave results unaffected by xuv self-absorption, the signal-to-noise ratio was unacceptably low. Moreover, these targets tended to be easily destroyed after a few shots of laser irradiation. Targets of width larger than 1 mm did not have this problem, but it was clear that there was xuv self-absorption close to the target. As a compromise, the targets were fabricated at 300–500 μm for the measurement of the branching ratio. Targets of larger widths were used only to demonstrate the xuv self-absorption. The target had several steps (typically six) as shown in Fig. 1, and plasmas at various distances from the target surface could be observed by moving the target up and down with a micrometer with vacuum feedthrough. The distance from observation region to target surface increased by 200 μm with each step. The radiation emitted from the plasma first passed through a narrow slit S of 200 μm width, which was fixed in the target chamber at a distance of 15 mm from the target. The width of this slit S was also chosen as a trade-off between the signal-to-noise ratio and the spatial resolution of the measurement.

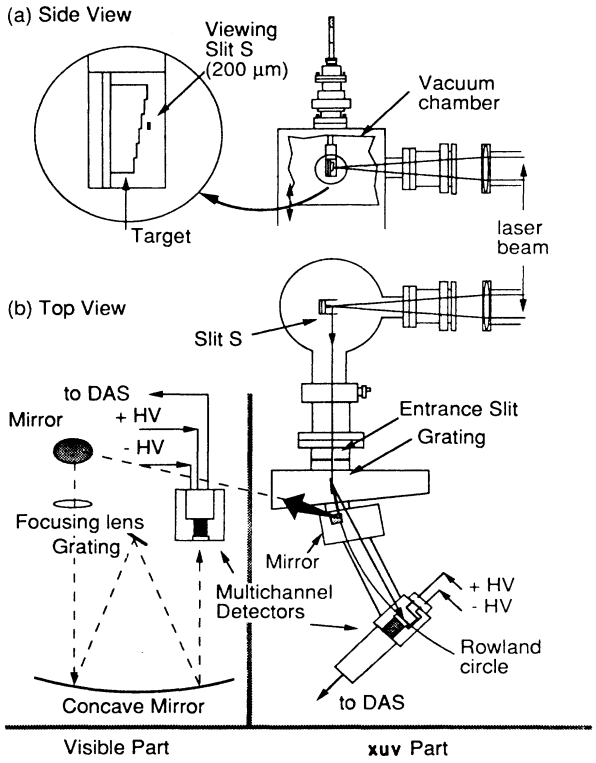

FIG. 1. Experimental setup. (DAS is the data acquisition system and HV is high voltage.)

Since the distance between the slit S and the target surface varied by 200 μm, we chose the slit width S to be 200 μm as well. A larger slit width would give a better signal-to-noise ratio, but would also nullify the resolution provided by the target steps.

We used one or more of the lasers to produce the plasma. For the measurement of the branching ratio, we primarily used the CO_2 laser for producing plasmas with density $N_e < 10^{19}$ cm^{-3}, the ruby laser for $N_e < 10^{21}$ cm^{-3}, and the XeCl laser for $N_e < 10^{22}$ cm^{-3}.

In order to record the xuv and the visible spectra simultaneously from exactly the same plasma region, we used a specially constructed xuv-visible duomultichannel spectrometer. The radiation emitted by the plasma, after passing through the narrow slit S in the target chamber, enters the spectrometer through the entrance slit as shown in Fig. 1(b). Here again, it was necessary to optimize the width of the entrance slit for the maximum signal-to-noise ratio as well as the maximum signal for the visible spectrum. The typical width was set between 50 and 200 μm, depending on how well the line of our interest was separated from adjacent lines, and provided

TABLE I. Characteristics of the lasers used in this work.

Laser	Energy (J)	Pulse (ns)	Beam shape	Beam size	Wavelength
CO_2	10	150	Annular	3.75 in. (OD[a]), 1.75 in. (ID[b])	10.6 μm
Ruby	5	20	Circular	1 in. diameter	694 nm
XeCl	1	40	Rectangular	3×2 cm^2	308 nm

[a] Outer diameter.
[b] Inner diameter.

the xuv spectrometer resolution of 0.8–3.0 Å.

The grating separates the incident beam into the zeroth-, first-, and other higher-order diffractions. 600 or 1200 rulings per mm grating was used. The zeroth-order beam is sent to the visible multichannel spectrometer by the periscope which consists of a small mirror placed immediately after the grating in the vacuum, and another large mirror in the air in front of the focusing lens. Other higher-order beams reach the xuv multichannel detector directly. The small mirror was placed very carefully at the point of focus of the zeroth-order beam on the Rowland circle. Special precautions were taken in order not to block the path of the first-order beam containing the wavelengths of our interest. The focusing lens in front of the visible spectrometer focuses this zeroth-order beam to a narrow image of the xuv entrance slit at the place of the visible entrance slit. Both the entrance slit and the exit slit were removed from the visible spectrometer. The position of the focusing lens was adjusted for the minimum instrumental broadening on the detector. The full width at half-maximum (FWHM) of the mercury 5461 Å line was 1.6 Å, which we took as the instrumental broadening of the visible spectrometer.

The electron density was measured from Stark broadening of the C IV 5801.5-Å line using the quasistatic approximation $\Delta\lambda_s = aN_e^{2/3}$.[11] Instrumental broadening $\Delta\lambda_{\text{inst}} = 1.6$ Å was subtracted from the linewidth measured from the spectra. The coefficient a was determined from the measured value of $\Delta\lambda_s = 6$ Å related to data at 1.5×10^{18} cm^{-3} in Ref. 12.

In Fig. 3 are shown the spectra obtained in the vicinity of C IV 312 and 5801–5812 Å (shaded lines) at distances of 0.2 and 0.4 mm from the target, respectively. The grotrian diagram for C IV is shown in Fig. 2(a). The branching-ratio R was calculated from the ratio of the

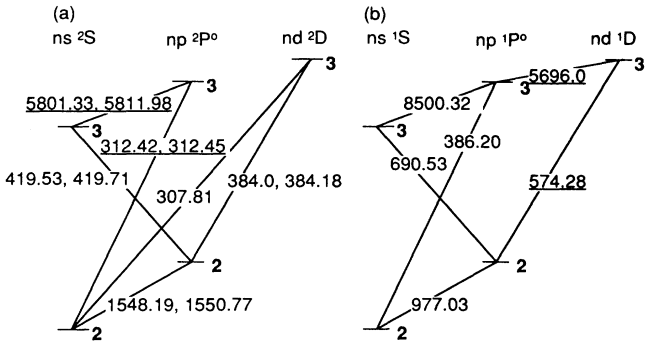

FIG. 2. Grotrian diagrams for (a) C IV and (b) C III. The branching pairs measured in this experiments are marked by underlines.

shaded areas of the visible and the xuv lines, which gave $R = 0.92$ at $d = 0.2$ mm and $R = 2.9$ at $d = 0.4$ mm. The xuv line was instrumentally broadened mostly due to the entrance slit of 200-μm width on the spectrometer. The broadening of the visible line is mostly due to the Stark effect. As shown in Table II, the contribution of the natural linewidth and the Doppler broadening (assuming $T_e \approx 5$ eV) to the line broadening is negligible in all cases of our interest. Results from the measurement of changes in the branching ratio of C IV ions were presented in our earlier work.[10] In this paper we add a more detailed analysis of the line profiles and present new results from the supplementary testing experiments.

To justify the claim made in this experiment, it is crucial to prove that the branching ratio we measured was truly the ratio of the spontaneous-emission intensities and

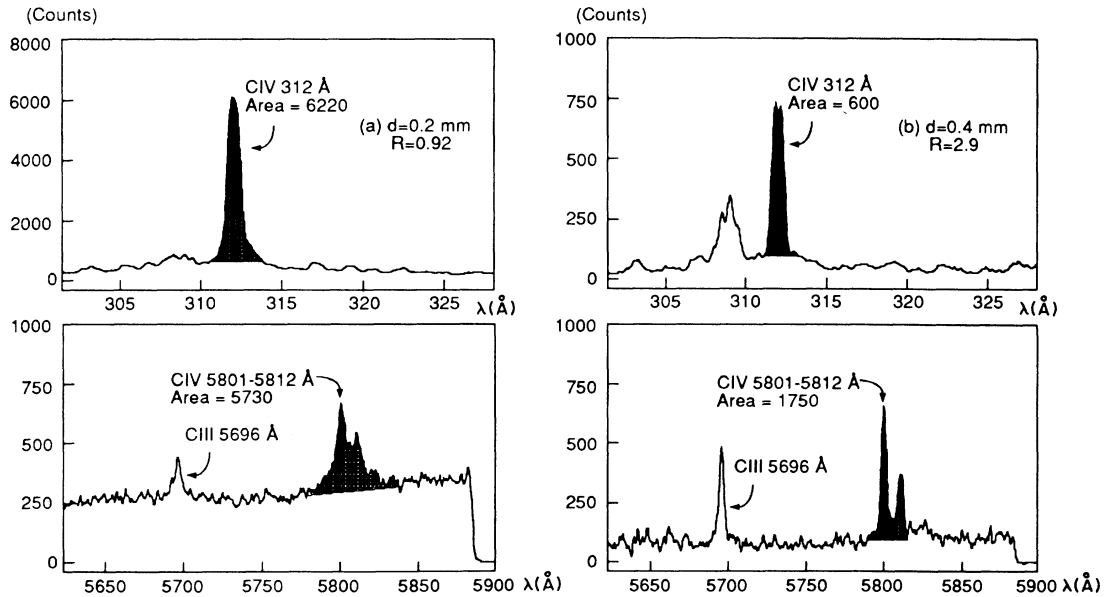

FIG. 3. xuv and visible spectra of C IV taken simultaneously at distances of (a) $d = 0.2$ and (b) $d = 0.4$ mm from the target surface. The upper ones are xuv spectra and the lower ones are visible spectra.

TABLE II. The list of the line pairs whose branching ratios were measured in this work. $\Delta\lambda_N$ is the natural linewidth and $\Delta\lambda_D$ is the Doppler-broadened linewidth.

Ion	λ (Å)	Transition	A_{ki} (10^8 sec^{-1})	$\Delta\lambda_N$ (Å)	$\Delta\lambda_D$ (Å)
C IV	312.42–312.46	$3p$-$2s$	45.6	1.5×10^{-4}	0.014
	5801.5–5812.1	$3p$-$3s$	0.32	5.1×10^{-2}	0.27
C III	574.28	$3d$-$2p$	63	6.9×10^{-4}	0.026
	5696.0	$3d$-$3p$	0.50	6.9×10^{-2}	0.26
N V	209.27–209.30	$3p$-$2s$	120	1.8×10^{-4}	0.009
	4603.8–4619.9	$3p$-$3s$	0.413	8.5×10^{-2}	0.20

that the measurement was not affected by absorption or cutoff. The evidence that visible lines were not absorbed (or self-absorbed) is manifested in the near-perfect coincidence of the experimentally measured profile of C IV 5801 Å ($J=\frac{3}{2}$) and 5812 Å ($J=\frac{1}{2}$) and the combination of their Lorentzian profiles with a 2:1 intensity ratio. Figure 4 shows the fitting of the experimental data and the combination of Lorentzian profiles of C IV visible lines shown in Fig. 3. If there had been any absorption, the intensity ratio of the two lines would be smaller than the theoretical ratio of 2:1, since a stronger line would be more absorbed. This analysis strongly suggests that the plasma was optically thin for visible transitions. Absorption or self-absorption of xuv lines would tend to increase the branching ratio $R=I_{\rm vis}/I_{\rm xuv}$ and thus decrease the effect of quenching of the A coefficient of the visible transition.

As another remark on the analysis of the visible spectrum, we discuss uncertainties arising from the integration of the experimental profile used in the calculation of the branching-ratio R. If the line is very broad, the boundary of the line profile to be integrated becomes less distinct, and this may introduce error in the integration. This can be quite a serious problem in the correct estimation of the total intensity when the background level is noisy or not smooth. Therefore, it is important to choose the end points of integration very carefully (and conservatively) in order not to underestimate the intensity of the visible transition at high plasma density. However, it is our belief that the uncertainty in integration cannot account for the observed change in the branching ratio. Figure 5 shows three cases of integration with different end points and the comparison of these values with the theoretical curve based on the assumption that the line profiles are Lorentzian. The end points we used for the actual calculation of the area are the same as the end points of the tentative background level line marked 1. This shows that as long as this tentative background level line does not deviate visibly from the adjacent background level, the error in the integration of the profile is relatively small compared to the observed change in branching ratio.

To prove experimentally that the measurement was not affected by absorption, we also measured the transmis-

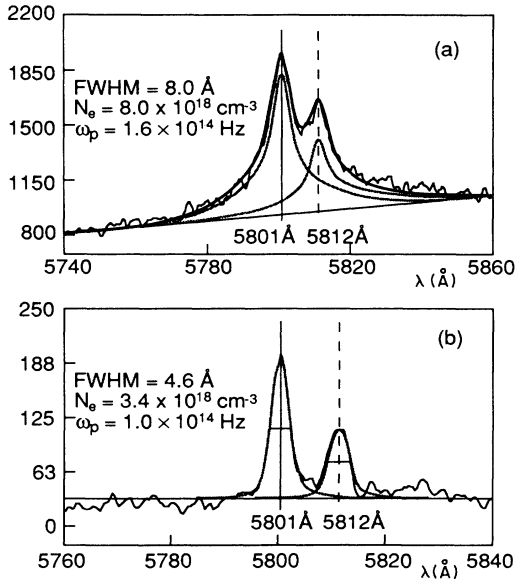

FIG. 4. Fitting of the experimental data with the convolution of Lorentzian profiles of C IV 5801 Å and 5812 Å lines. (a) $d=0.2$ mm, $R=0.92$, (b) $d=0.4$ mm, $R=2.9$.

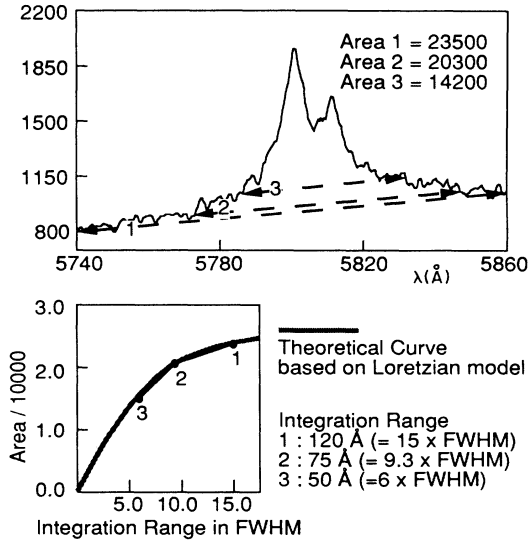

FIG. 5. Estimation of error in integrating the line profile. The integration was done below the experimental profile and above the tentative background levels marked as dashed lines.

sivity of the plasma at various distances from the target. The experimental setup is shown in Fig. 6(a). The CO_2 laser beam was split into two identical beams by a NaCl window tilted at $\approx 30°$ with respect to the plane perpendicular to the beam axis. The resulting separation of the two plasmas created at the target 50 cm away from the focusing lens was 2.5 mm. The narrower target was 500-μm wide and the other target was 2.7-mm wide. The positions of the beams were adjusted so that the plasmas were created at the center of the left target and at the edge of the right target. To measure the transmissivity of the plasma on the left target, we first obtained spectra from the left plasma and the right plasma separately by blocking one of the laser beams. Then we obtained the spectra with two plasmas. The measured intensities are denoted by I_1 (left plasma), I_2 (right plasma), and I_{1+2} (together), respectively in Fig. 6. The transmissivity T was taken to be

$$T = \frac{I_{1+2} - I_1}{I_2}.$$

The result shows that there was no significant absorption of either the xuv or the visible light by the plasma created on the thin left target. This experiment demonstrates that the measurement of the change of the branching ratio was not affected by absorption (or self-absorption) at all.

We observed the same effect of quenching of spontaneous emission in ruby-laser-produced C IV plasmas of higher density as well as in other ions, namely, in C III and N V produced by the CO_2 laser. The grotrian diagram for C III is shown in Fig. 2(b). Figure 7 shows the spectra obtained in the vicinity of C III 574 and 5696 Å (shaded lines) at distances of 0.6 and 1.3 mm from the target, respectively. The branching ratio R was calculated from the ratio of the shaded areas of the visible and the xuv lines. It is shown clearly in Fig. 7 that while the xuv intensity drops by a factor of 4, the visible intensity even increases slightly as the distance d increases from 0.6 to 1.3 mm. The result of the measurement for C III is

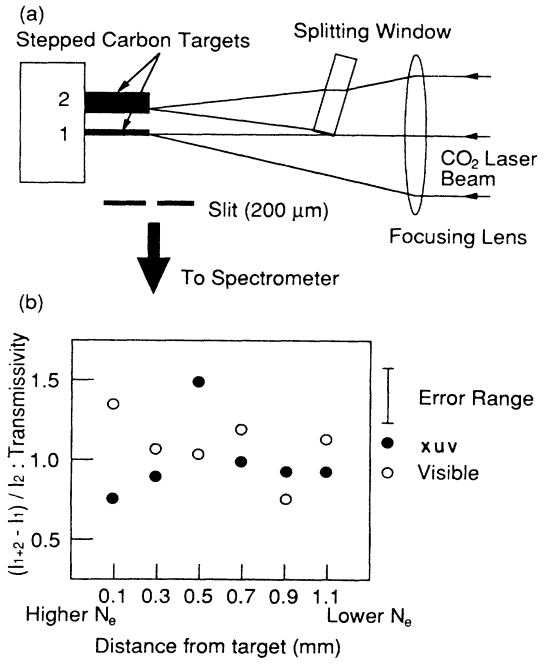

FIG. 6. Measurement of absorption: (a) experimental setup and (b) transmissivity of the plasma created on the narrow target as a function of distance from the target.

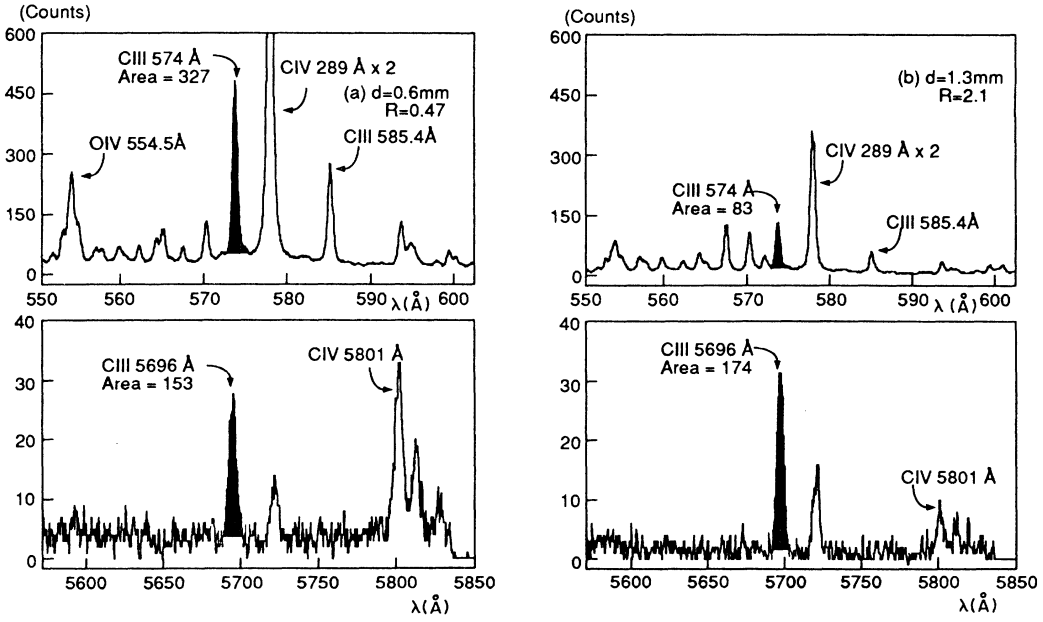

FIG. 7. xuv and visible spectra of C III taken simultaneously at distances of (a) $d=0.6$ and (b) $d=1.3$ mm from the target surface. The upper ones are xuv spectra and the lower ones are visible spectra.

presented in Fig. 8. We also measured the changes in the branching ratio for the C IV 312 and 5801–5812 Å lines with the ruby laser and N V 209 and 4603–4602 Å lines with the CO_2 laser. The results are shown in Figs. 9 and 10. In ruby-laser-produced plasmas, we could observe larger changes in the branching ratio due to higher N_e as compared with CO_2-laser-produced plasmas.

Measurements of the branching ratio between two transitions that share the same upper level is independent of several factors concerning the population changes that could affect the line intensities. Here lies the simplicity of the principle involved in this experiment. Even though the measurement of the temporal behavior of the lines can be of assistance in understanding the change of the branching ratio, it was not deemed to be essential. The decay time of a transition is, except for the resonance transitions, not equal to the reciprocal of the corresponding A coefficient but to the radiative lifetime of an excited level, which is given by the reciprocal of the sum of all the transition probabilities, i.e.,

$$\tau_i = \left[\sum_{k,k\neq i} A_{ik} + \sum_k N_e S^e_{ik} + \cdots \right]^{-1} .$$

Hence, all the transitions that branch from the same upper level should have the same temporal behavior but with different amplitudes proportional to the A coefficients. Therefore, assuming the plasma density was constant while the emission lasted so that the A coefficients did not change, we would have

$$\frac{N_3(t_i)A_{32}\Delta t_i}{N_3(t_i)A_{31}\Delta t_i} = C , \tag{2}$$

where C is a constant and $N_3(t_i)$ is the upper-level population at time t_i and Δt_i is the incremental time interval. If we take $\Delta t_i \rightarrow 0$ and integrate over time, Eqs. (1) and (2) will give

$$\frac{I^T_{32}}{I^T_{31}} = \frac{\int I_{32}(t)dt}{\int I_{31}(t)dt} = \frac{k_{32}}{k_{31}} C ,$$

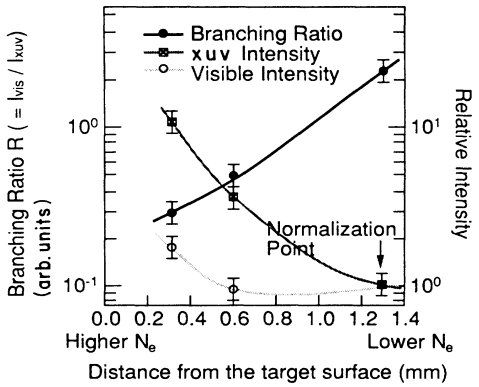

FIG. 8. Branching ratio $R = I_{vis}/I_{xuv}$ for C III 574- and 5696-Å lines as a function of distance from the target surface. Note that even though the xuv line intensity increases sharply near the target, the visible line intensity does not change very much.

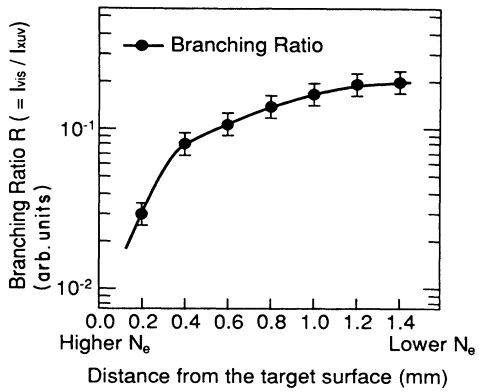

FIG. 9. Branching ratio $R = I_{vis}/I_{xuv}$ for N V 209- and 4603–4620-Å lines as a function of distance from the target surface. The plasma was produced by a CO_2 laser.

which is also constant. I^T_{32} and I^T_{31} are the time-integrated intensities. This shows that change of the branching-ratio R can be deduced from the change of the ratio of the time-integrated intensities alone.

III. THEORY

The theoretical effort has been going on since we obtained the preliminary results from the experiments measuring the branching ratio in C IV. However, there does not yet exist a theoretical model that can clearly and unequivocally explain this phenomenon. In this section, we describe our initial unsuccessful attempt, and then go on with a suggestion for possible future approaches.

We first speculated that the screening of the atomic potential by the surrounding plasma could modify the Coulomb field experienced by the electron and thus significantly change the transition probabilities. Several authors[13] have tried to obtain solutions to the Schrödinger equation for a particle in a screened Coulomb potential. Roussell and O'Connell calculated the spontaneous-emission probabilities in the dipole ap-

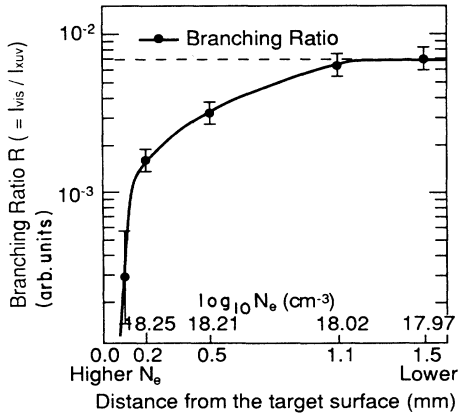

FIG. 10. Branching ratio $R = I_{vis}/I_{xuv}$ for C IV 312- and 5801–5812-Å lines as a function of distance from the target surface. The plasma was produced by a ruby laser for higher electron density ($N_e < 10^{21}$ cm^{-3}).

proximation as a function of Debye-Hückle screening length r_D for a hydrogen atom ($Z=1$) and showed that the spontaneous-emission probabilities began to drop sharply at $r_D=50a_0$, where a_0 is the Bohr radius.

In our case, the Schrödinger equation was solved numerically for C IV ions in the electric potential of the surrounding plasma. This potential was approximated by using the Debye radius $r_D \propto N_e^{-1/2}$, assuming T_e, the electron temperature, to be constant. The transitions of the valence electron were assumed to occur in the internal potential of two bound electrons ($1s^2$), approximated by a uniform charge cloud of radius R_0 and influenced by the external field. Therefore, the potential $V(r)$ was given by

$$V(r)=\begin{cases}\left\{\dfrac{Z'e^2}{2R_0}\left[3-\left[\dfrac{r}{R_0}\right]^2\right]-\dfrac{Ze^2}{r}\right\}e^{-R_0/r_D} & \text{if } r\le R_0\\ -\left[\dfrac{(Z-Z')e^2}{r}\right]e^{-r/r_D}, & \text{otherwise}\end{cases}$$

where e is the electron charge, r is the distance from the center of the charge cloud, $Z=6$ and $Z'=2$ for C IV, and R_0 was taken to be much smaller than r_D. Once the eigenfunctions were obtained by solving the Schrödinger equation, it was straightforward to obtain the branching ratio between the two transitions. In the dipole approximation, the Einstein A coefficients are given by

$$A(nl\rightarrow n'l')=\frac{4|\Delta E|^3}{3(2l+1)}S(nl,n'l')\ ,$$

where

$$S(nl,n'l')=\sum_{m,m'}|\langle nlm|\mathbf{d}|n'l'm'\rangle|^2\ .$$

The theoretical branching ratio R between the two transitions, $n_3l_3\rightarrow n_2l_2$ and $n_3l_3\rightarrow n_1l_1$, is then given by

$$R=\frac{A(n_3l_3\rightarrow n_2l_2)}{A(n_3l_3\rightarrow n_1l_1)}\ .$$

Figure 11 shows the results obtained for the cases ($5p\rightarrow 4s, 5p\rightarrow 1s$) of the hydrogen atom ($Z=1, Z'=0$) and ($3p\rightarrow 3s, 3p\rightarrow 2s$) of the C IV ion ($Z=6, Z'=2$) as functions of the Debye radius r_D. For the transitions between lower-lying states in the hydrogen atom, we obtain the same results as Roussell and O'Connell. As r_D approaches $10a_0$, the branching ratio begins to increase very rapidly for the C IV ion in contrast to the hydrogen atom. For hydrogenic ions ($Z>1$), the higher the Z number, the less drastic was this effect. The main cause for the change in C IV was the changes in the transition strength $S(nl\rightarrow n'l')$, while in the case of the hydrogen atom, it was the shift of energy levels. This result is not consistent with the experimental results in that no line shift was observed with increasing electron density, i.e., with decreasing Debye radius. This inconsistency clearly indicates that (1) the Debye-Hückle potential is not valid in our case since the plasma parameter

$$g=nr_D^3$$

is not much larger than 1, and/or (2) the electron density

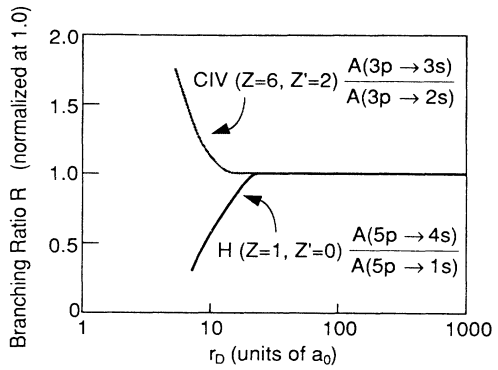

FIG. 11. Theoretical branching ratio R obtained by solving the Schrödinger equation with Debye-Hückel screened Coulomb potential for C IV ($3p\rightarrow 3s$ and $3p\rightarrow 2s$) and H ($5p\rightarrow 4s$ and $5p\rightarrow 1s$) as functions of the Debye radius r_D.

is still too low for the screening effect to become important. Assuming $T_e\approx 5$ eV and $N_e\le 10^{19}$ cm^{-3}, we have $r_D\ge 100a_0$ and $g\ge 1.5$. r_D and g become larger as the electron density decreases if T_e is constant. This is far away from the region where the screening of the potential can alter the transition probability significantly, and we conclude that the quenching of the Einstein A coefficients as observed in the experiment is due to some cause other than the screening of the static Coulomb potential by the surrounding plasma.

A different approach to the development of a theoretical model has been the modification of the Weisskopf-Wigner (WW) approximation of exponential decay of excited atoms.[14–17] Reference 15 is essentially an extension of the WW in the sense that the coupling between the first continuum of states to which the excited atom initially decays and the second continuum was taken into account. In this case, the decay rate of the initial excited state can decrease if the first continuum of states is itself unstable and coupled to a still lower-lying continuum of states. Even though the probability that the excited state stays there remains exponential, the decay rate may be changed. If only the second continuum were considered in addition to the first continuum and if the coupling strengths V_{32} and V_{21} could be factored as $V_{32}=F_0G_0$ and $V_{21}=F_1G_1$, the modified decay rate γ would be[17]

$$\gamma=\frac{\gamma_{GR}}{1+H_1}\ , \tag{3}$$

where γ_{GR} is the Fermi golden rule rate, and H_1 is an intrinsically positive quantity proportional to the square of the coupling strength V_{21}.

We are presently following this line of approach and exploring the possibility of relating the rapid depletion of the lower level of transition by collisional deexcitation to the suppression of radiative decay from the initially excited level 3 (see Fig. 12). The transition between levels 2 and 1 is forbidden in the dipole approximation, and the level 2 would be metastable unless provided with other channels of decay. The coupling between the levels 2 and

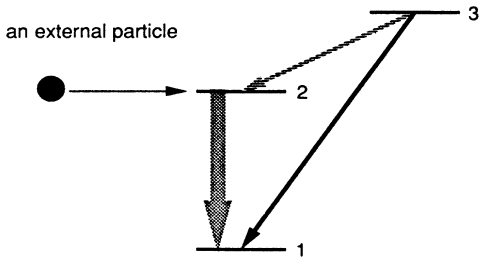

FIG. 12. Hypothetical theory: radiative transition may be quenched when the coupling between levels 2 and 1 becomes large through the collisional deexcitation by electrons.

1 is provided by collisional deexcitation whose rate will increase linearly with the electron density N_e.

IV. CONCLUSION

We described experiments that focused on the change of branching ratio in high-density plasmas as well as our theoretical efforts to explain the phenomenon. Various possible explanations other than the decrease of Einstein A coefficients in the high-density regime were judged to be unfounded. The result presented in this paper is expected to have a significant impact on other areas of research. For example, in the spectroscopic studies of fusion plasmas, the intensities of several lines are used to determine the relative population of different energy levels, plasma temperature, and composition of the plasma in terms of ionization stage and impurity concentration, etc. If the Einstein A coefficients of some or all of the lines are considerably different from the values in the low-density limit, the rate equation would have to be modified in order to take into account the quenching effect.

At this time, we still lack a satisfactory theoretical explanation of why the branching ratio, hence the Einstein A coefficient, changes in high-density plasmas, and maybe the formalism developed earlier by Barrat and Cohen-Tannoudji[18] for optical pumping can also be applied to our strongly collisional plasma.

ACKNOWLEDGMENTS

The authors would like to thank I. Bernstein, H. Furth, H. Griem, R. Kulsrud, J. Lebowitz, M. Littman, T. McIlrath, C. Oberman, J. L. Schwob, C. Skinner, S. Susskind, E. Valeo, and A. Wouters for the stimulating discussions and suggestions of a number of supplementary testing experiments. This work was supported by U.S. Department of Energy Advanced Energy Projects of Basic Energy Sciences, Contract No. KC-05-01. This work was performed at the Princeton Plasma Physics Laboratory, which operates under U.S. Department of Energy Contract No. DE-ACO2-76CHO3073.

---

*Present address: Nagoya University, Nagoya, Japan.
†Also at Department of Mechanical and Aerospace Engineering, Princeton University.

[1]V. Weisskopf and E. Wigner, Z. Phys. **63**, 54 (1930) [translated in *Atomic Spectra,* by W. R. Hindmarsh (Pergamon, London, 1967), p. 304].
[2]M. D. Crisp and E. T. Jaynes, Phys. Rev. **179**, 1253 (1969).
[3]A. O. Barut and J. F. van Huele, Phys. Rev. A **32**, 3187 (1987).
[4]E. M. Purcell, Phys. Rev. **69**, 681 (1946).
[5]D. Kleppner, Phys. Rev. Lett. **47**, 233 (1981).
[6]R. G. Hulet, E. S. Hilfer, and D. Kleppner, Phys. Rev. Lett. **55**, 2137 (1985).
[7]W. Jhe *et al.*, Phys. Rev. Lett. **58**, 666 (1987).
[8]G. Gabrielse and H. Dehmelt, Phys. Rev. Lett. **55**, 67 (1985).
[9]E. Yablonovitch, Phys. Rev. Lett. **58**, 2059 (1987).
[10]Y. Chung, P. Lemaire, and S. Suckewer, Phys. Rev. Lett. **60**, 1122 (1988).
[11]H. Griem, *Plasma Spectroscopy* (McGraw-Hill, New York, 1964), p. 229.
[12]M. A. El-Farra and T. P. Hughes, J. Quant. Spectrosc. Radiat. Transfer **30**, 335 (1983).
[13]See K. M. Roussell and R. F. O'Connell, Phys. Rev. A **9(1)**, 52 (1974) and references therein.
[14]S. D. Druger, J. Chem. Phys. **73**, 2287 (1980).
[15]E. J. Robinson, Phys. Rev. Lett. **57**, 1281 (1986).
[16]Z. Deng and J. H. Eberly, Phys. Rev. Lett. **53**, 1810 (1984).
[17]Z. Deng and J. H. Eberly, Phys. Rev. Lett. **58**, 618 (1987).
[18]J. P. Barrat and C. Cohen-Tannoudji, J. Phys. (Paris) **22**, 329 (1961).